Molecular Structure, Conformational Analysis, and Structure−Activity Studies of Dendrotoxin and Its Homologues Using Molecular Mechanics and Molecular Dynamics Techniques

Panchanadam Swaminathan,*,† Meena Hariharan,‡,§ Ramachandran Murali,⊥ and Chandra U. Singh||

Department of Chemistry, Wyeth-Ayerst Research, CN-8000, Princeton, New Jersey 08543-8000, Department of Molecular Biology, Scripps Clinic and Research Foundation, La Jolla, California 92037, Department of Pathology and Laboratory of Medicine, University of Pennsylvania, Philadelphia, Pennsylvania 19104, and A. M. Technologies Inc., 14785 Omicron Drive, San Antonio, Texas 78245

Received August 3, 1995[⊗]

Three-dimensional structures of Dendrotoxin (DtX), Toxin-I (DpI), and Toxin-K (DpK) were determined using molecular mechanics and molecular dynamics techniques. The overall molecular conformation and protein folding of the three dendrotoxins are very similar to the published crystal structures of bovine pancreatic trypsin inhibitor (BPTI) and α-DtX. Major secondary structural regions of the dendrotoxins are stable without much fluctuation during the dynamics simulation; the regions corresponding to the turns and bends (rich in lysines and arginines) exhibit more fluctuations. The conformational angles and the $C^{\alpha}\cdots C^{\alpha'}$ distances of the three disulfides (in each of the dendrotoxins) are different from each other. Comparative model building studies, involving the dendrotoxins and the proteinases, reveal that the key interactions (observed in BPTI−trypsin complex) needed for anti-protease activity are absent due to structural differences between the dendrotoxins and BPTI at the anti-protease loop; this explains the inability of the dendrotoxins to inhibit proteinases. The model also suggests that the solvent-exposed β-turn region, rich in lysines (residues 26−28), might bind directly to the extracellular anionic sites of the receptors (K^+ channels) by ionic interactions. The strikingly homologous cysteine distribution (Cys-x-x-x-Cys) in DtX, DpI, and DpK, at the C-terminus, induces the occurrence of a characteristic conformational motif, consisting of an α-helix (in an amphiphilic environment) stabilized by two disulfides, one involving a cysteine at the β-strand, and the other at the N-terminus. This amphiphilic secondary structural element seems to provide the rigid frame work needed for exposing the proposed active site region of the dendrotoxins to the anionic sites of the K^+ channel receptors.

Introduction

Dendrotoxins belong to the family of snake toxins found in the venom of African mamba snakes (*Dendroaspis* species). Among the members of this group of toxins are Dendrotoxin, isolated form African green mamba snakes *Dendroaspis angusticeps*, [1−2] Toxin-I, from African black mamba *Dendroaspis polylepis polylepis*-I,[3] and Toxin-K, from *Dendroaspis polylepis polylepis*-K.[3] Dendrotoxin (DtX), Toxin-I (DpI), and Toxin-K (DpK) are the most intensely studied snake toxins.

Dendrotoxins (collectively refers to DtX, DpI, and DpK in this article) enhance the neuromuscular transmission *in vitro* and augment the release of acetylcholine from the nerve endings. They do not have any enzyme activity and do not damage the nerve terminal. Besides, the dendrotoxins are more potent than 3,4-diaminopyridine at enhancing the responses of chick biventor cervicis nerve muscle preparations.[4] *In vivo*, their notable effect is to produce excessive muscular activity *via* neuromuscular synapses. The facilitatory actions of the dendrotoxins, at the peripheral[4] and central[5−7] synapses, are due to their capacity to inhibit the A current[8] in hippocampal pyramidal cells and other fast activating aminopyridine sensitive voltage-gated K^+ conductances in a variety of neurons.[7−10] Dendrotoxins produce excessive convulsive action by specifically blocking voltage sensitive K^+ channels.[11]

β-Bungarotoxin, a similar neurotoxin from the venom of Taiwan krait, *Bungarus multicinctus*, has been shown to inhibit potassium currents at the motor nerve endings and thus possess facilitatory effects at the mouse neuromuscular junction.[12,13] Unlike the dendrotoxins, β-bungarotoxin contains two polypeptide chains A and B. The longer A chain has been shown to possess Ca^{2+} dependent phospholipase activity, while the shorter B chain is homologous to the Kunitz type proteinase inhibitors without the proteinase-inhibiting activity. Thus, the B chain of β-bungarotoxin is similar to the dendrotoxins. Likewise, mast-cell degranulating (MCD) peptide, isolated from the venom of European honey bee *Apis mellifera*, has been shown to block a voltage dependent K^+ conductance in sensory neurons.[14] Using radiolabeled binding techniques, it has been shown[15] that the dendrotoxins inhibited the binding of radioiodinated β-bungarotoxin in Krebs medium with high potency by a complex noncompetitive mechanism. MCD peptide has been shown to inhibit noncompetitively the binding of both radiolabeled dendrotoxin and β-bungarotoxin. A speculative model has also been proposed for the binding of dendrotoxin/β-bungarotoxin/mast-cell degranulating peptide.[15] A clear understanding of the structural features of the highly homologous dendrotoxins will shed light on understanding the mechanism

* Author to whom correspondence should be addressed at 1436 Joel Dr., Ambler, PA 19002.
† Wyeth-Ayerst Research.
‡ Scripps Clinic and Research Foundation.
§ Present address: Department of Biochemistry, University of Minnesota, St. Paul, MN 55108.
⊥ University of Pennyslvania.
|| A. M. Technologies Inc.
⊗ Abstract published in *Advance ACS Abstracts,* May 1, 1996.

S0022-2623(95)00579-6 CCC: $12.00

Table 1. Comparison of Amino Acid Sequences of DtX, DpI, DpK, B Chain of β-Bungarotoxin, and BPTI

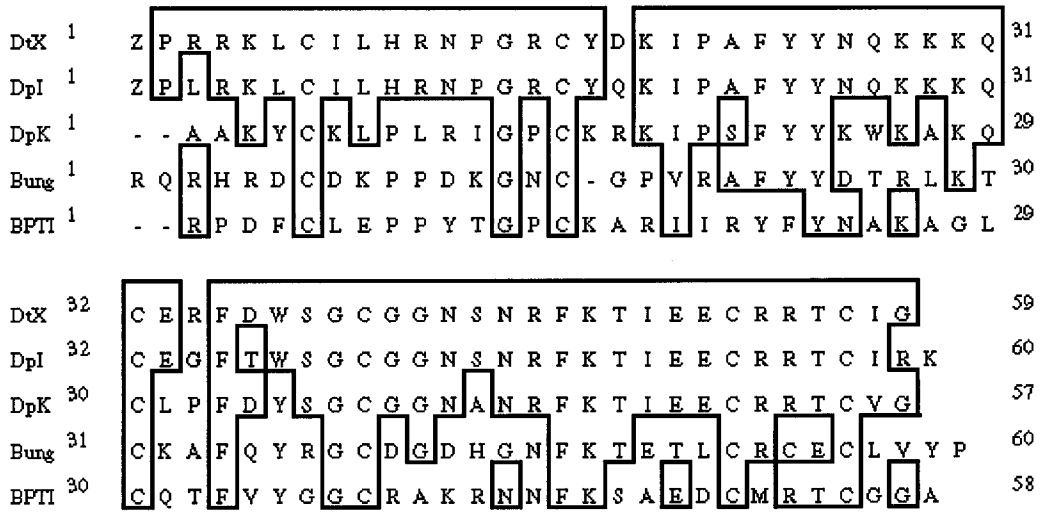

Standard single letter amino acid abbreviations are used: A-alanine, C-cysteine, D-aspartic acid, E-glutamic acid, F-phenylalanine, G-glycine, H-histidine, I-isoleucine, K-lysine, L-leucine, M-methionine, N-asparagine, P-proline, Q-glutamine, R-arginine, S-serine, T-threonine, V-valine, W-tryptophan, Y-tyrosine, Z-pyroglutamic acid.

of action of these toxins on the K^+ channels. This can lead us to characterizing the architecture and the properties of K^+ channels.

A critical analysis of the sequence of the toxins indicates that the dendrotoxins belong to the Kunitz proteinase inhibitor family.[16,17] Bovine pancreatic trypsin inhibitor (referred to as BPTI), also a member of the Kunitz family, has been studied in greater detail using X-ray crystallographic techniques.[18−20] The primary structure of BPTI is homologous to the dendrotoxins. The circular dichroism spectra of the dendrotoxins and BPTI are very similar. However, the dendrotoxins are the only members of the Kunitz family that do not inhibit the common proteases like trypsin and chymotrypsin but enhance the neuromuscular activity and interfere with the potassium channels. In contrast, several other inhibitor homologues from the mamba venom and other snake venom have been shown to exhibit anti-protease activity, but do not interfere with the potassium channels or neuromuscular transmission.[21]

We have initiated the work on the structural features of the dendrotoxins in 1988 as part of our on-going project on developing ion-channel modulators, here at Wyeth-Ayerst Research. Preliminary results of our analysis were reported elsewhere.[22,23] Previously the X-ray crystal structure of α-DtX at 2.5 Å resolution[24] was reported. More recently, tertiary structures of DpI[25] and DpK[26] based on NMR spectral data have been published. These results indicate that the three-dimensional structure and chain folding of the dendrotoxins are similar to that of BPTI, which is in agreement with our earlier finding.[22,23] In this report, we describe the interactions between the proteinases (trypsin and kallikrein) and the dendrotoxins using comparative molecular modeling. The model provides an insight into the possible site of action for the channel-blocking properties of these toxins.

Methods

DtX, DpI, and DpK have 57−60 amino acid residues (Table 1). All of them contain six cysteines which are linked to form three disulfide bridges. The number of amino acid residues between the first and the last cysteine is exactly 51 in the dendrotoxins reported in Table 1. The order of disulfide formation between these cysteines is also preserved in all the structures. This unique property makes it easy to align the sequence of BPTI and those of the dendrotoxins in building the models of DtX, DpI, and DpK. The dendrotoxins contain more than five arginines and lysines in their sequence. There is a high degree of homology between these toxins. All these clearly suggested that the three-dimensional folding and the architecture of these toxins should be very similar[16] to each other.

Three-dimensional trial structures of DtX, DpI, and DpK were generated starting with the X-ray crystal structure of BPTI, determined at 1.5 Å resolution.[20] During this procedure, we modified the amino acids one at a time to arrive at the model of the dendrotoxins. Typically as soon as one amino acid residue of BPTI was modified to match the sequence of the dendrotoxins, the side chain conformation was altered using the rotatable bonds so that any bad contacts with either the backbone or the neighboring residue of the protein could be removed. In this way, the amino acid residues of BPTI sequence were modified to match the sequence of the dendrotoxins. The model building of the dendrotoxins was carried out on a silicon graphics workstation (SGI-4D/380 VGX) using SYBYL program.[27] The trial models of the dendrotoxins were subjected to molecular mechanics minimization using AMBER.[28] Since the proteins under study carry a net positive charge, these were neutralized using counterions. This was done using the COUNTER module of AMBER. The charges on the atoms of pyroglutamic acid were calculated by *ab initio* methods using the STO-3G basis set using the program QUEST.[29,30] The charges on the other amino acids were taken from the literature.[31] During the initial stages the proteins were minimized in vacuum.

Solvent molecules are known to play a critical role on the equilibrium conformation of the protein structures.[32−35] All the three proteins studied in this report contain a significant number of lysines and arginines on the surface of the proteins. In order to remove the extreme torsional fluctuations of the side chains of the charged residues, such as lysines and arginines, dynamic simulations were carried out in the solvent water. In the absence of the surrounding water molecules, the charged side chains tend to fall back on the backbone of the proteins and can result in the overall shrinking of the proteins during dynamic simulation.

Each protein molecule and the counterions were solvated using the isolated spherical drop model. The molecules were placed in a solvent box made up of 64 cubes of 216 water molecules, and all the water molecules, which are within 3.6 Å of any protein atoms, were removed. All the solvent molecules, which are farther than 27.5 Å from the center of mass of the protein, were not included in the simulation. Approximately 5000 water molecules were used to surround the protein molecule and the counterions. The outer boundary of the spherical shell was defined by means of an artificial wall with a potential of the type W, defined as

$$W = \left\{ \frac{A_{i\text{wall}}}{(R_b - |r_i|)^{12}} - \frac{C_{i\text{wall}}}{(R_b - |r_i|)^6} \right\} + A(|r_i| - R_0) + B \quad (1)$$

where the constants $A_{i\text{wall}}$ and $C_{i\text{wall}}$ are computed as

$$A_{i\text{wall}} = \epsilon_{i\text{wall}}(R_{i\text{wall}})^{12} \qquad \text{and} \qquad C_{i\text{wall}} = 2\epsilon_{i\text{wall}}(R_{i\text{wall}})^6$$

This potential was developed to ensure that the molecules inside the sphere never escape and maintain a fully solvated system during molecular dynamics.

Here $\epsilon_{i\text{wall}} = (\epsilon_i \epsilon_{\text{wall}})^{1/2}$ and $R_{i\text{wall}} = (R_i + R_{\text{wall}})$, where ϵ_i is the well depth of atom i, R_i is the van der Waals radius of atom i, ϵ_{wall} is the well depth, and R_{wall} is the van der Waals radius for the wall. We have chosen the value of 0.1 kcal for the well depth and 1.25 Å for the radius for both atom i and the wall. The quantity $|r_i|$ is the distance between atom i and the center of the water sphere, and R_0 is the radius of the sphere. The quantities A, B, and R_b were determined by imposing the condition that W and dW/dr_i vanish at $|r_i| = R_0$. The restraining potential W was set to zero for $|r_i| < R_0$.

The entire structure with the water molecules was minimized for 5000 cycles by conjugate gradient method using the BORN module of AMBER.[28] A cutoff distance of 9 Å was used for calculating the nonbonded interactions. Before the molecular dynamics simulations were started, the structure was minimized for 100 cycles using the SHAKE algorithms. For molecular dynamics simulations, the system was gradually heated from 0 to 300 K. The equilibration was carried out at constant temperature 300 K for 10 ps with a time step of 0.001 ps. Classical dynamics calculations, without pressure monitoring, were carried out for 200 ps. Energy-related quantities and velocities were written out once every 1 ps and coordinates once every 0.4 ps. A constant dielectric of 1 was used for all the calculations. All bonds were constrained with a relative geometric tolerance for coordinate resetting of 0.0005 Å. All bond interactions were neglected. The energy and the temperature were monitored during dynamics, and the average temperature was around 300 K. The rms fluctuation of the total energy was within 0.6% of the total energies, and the temperature within 1 K.

In order to determine the nature of interactions between the proteases and the dendrotoxins, comparative model building was attempted. For this purpose, the published X-ray crystal structures of BPTI−trypsin[36] and BPTI−kallikrein complexes[37] were retrieved from the Brookhaven data bank. The backbone atoms of the dendrotoxins and those of BPTI fragments of the complexes, were fitted using SYBYL.[27] The fitted structures of the dendrotoxins were docked to the trypsin and the kallikrein structures. The complexes were neutralized using counterions, and a 27.5 Å cap of water was placed at the center of the toxin molecules. The system was minimized using the segment option, and all the residues within 28 Å from the center of the toxin molecule were considered as the active residues. The system was subjected to 40 ps of molecular dynamics and was further minimized for 8000 cycles using AMBER.[28] Figures 6 and 7 show the residues at the antiprotease site of DtX in complex with kallikrein and trypsin. Figures 8 and 9 show the α-carbon plots of the dendrotoxins in complex (based on comparative modeling) with the proteinases kallikrein and trypsin. All the energy minimizations and molecular dynamics calculations reported in this paper were carried out on a CRAY-YMP supercomputer at the Scripps Clinic and Research Foundation, La Jolla, CA.

Results and Discussion

Molecular Conformation. The residue numbering of the dendrotoxins follows the same scheme as that of BPTI in the following discussion. The protein folding and the overall conformations of DtX, DpI, and DpK are similar (Figures 3 and 4) to those of BPTI with minor differences. In all the structures, the residues occurring at the ends of the α-helices near the C-termini have an irregular conformation. All three structures have two antiparallel β-sheets and a short α-helix (4_{10} helix) near the carboxy terminal. In DtX, residues 20−24 and 29−33 form a double-stranded antiparallel β-sheet conformation. The (ϕ, ψ) values of the β-sheets are spread over all the values allowed for extended polypeptide chains (Figure 2a), resulting in a right-handed twist for the β-strands.[38] Residues 47−56 occur in a short α-helical conformation with mean (ϕ, ψ) values of (−69°, −43°). Amino acid residues 2−6 occur in (distorted) 3_{10} helix conformation with mean (ϕ, ψ) values of (−34°, −43°). It is interesting to note that the conformation of the amino acids at the N-terminal region is a random coil in the crystal structure of α-DtX.[24] In DpI, residues 18−24 and 29−35 occur in two antiparallel β-strands with a right-handed twist, as observed in DtX. A short α-helix (4_{10} helix) is observed near the carboxy terminal comprising of residues 48−56 with mean (ϕ, ψ) values (Figure 2b) of (−80°, −35°). Amino acid residues 2−6 (at the N-terminus) occur in a regular α-helix with mean (ϕ, ψ) of (−81°, −38°). Similarly in the case of DpK, residues 16−24 and 29−34 occur in antiparallel β-strands with a right-handed twist. Residues 48−54 at the carboxy terminus occur in an α-helical conformation with mean (ϕ, ψ) values (Figure 2c) of (−70°, −40°). It is interesting to note that the conformation of the amino acid residues (of DpK) near the N-terminus occurs in a random coil in contrast to the helical conformation observed in DtX and DpI structures. The dendrotoxins (including BPTI and crystal structure of α-DtX) contain a β-turn[39] occurring between the two antiparallel β-strands. In DtX, residues 25−28 occur in a β-turn conformation, while residues 25−30 of DpI and residues 25−28 of DpK occur in β-turn. Studies have shown that majority of these hairpin turns occur on the surface or the edge of the protein structures rather than on the interior. An analysis of the amino acid residues occurring in the hairpin turns shows that almost all the residues are hydrophilic in nature, which explains the occurrence of the bend on the edge or surface of the proteins rather than on the interior.[39]

Dendrotoxins are basic proteins with a net positive charge. DtX contains eight arginines, six lysines, two aspartates, and three glutamate residues. There is a concentration of positive charges (Arg 1, Arg 2, and Lys 3) near the N-terminus, (Arg 52, Arg 53, and Arg 57) near the C-terminus, and also at the β-turn (Lys 26, Lys 27, Lys 28) between the two β-strands. All of the negatively charged residues of DtX (Asp 16, Asp 32, Glu 31, Glu 49, and Glu 50) are located on one side of the pear-shaped molecule.

DpI contains seven arginines, seven lysines, and three glutamate residues. As in the case of DtX, there is a concentration of positively charged lysines at the turn between the two β-strands (Lys 26, Lys 27, Lys 28), near the C-terminus (Arg 52, Arg 53, Lys 57), and near the N-terminus (Arg 2 and Lys 3).

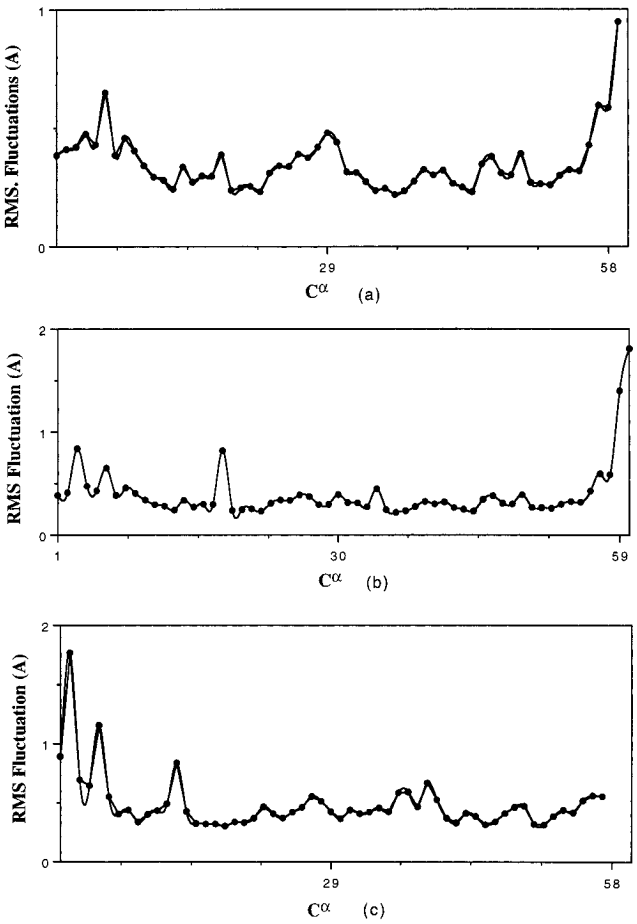

Figure 1. RMS fluctuations (Å) of C^{α} atoms of (a) DtX, (b) DpI, and (c) DpK. The numbers along the *x*-axis correspond to the residue numbers.

In DpK, there are five arginines, eight lysines, one aspartate, and two glutamate residues. Of these, Lys 17 forms a salt bridge with Asp 34, Arg 52 with Glu 49 and Arg 53 with Glu 50. The remaining arginines and lysines are distributed throughout the protein. As in the other two structures, the loop between the two β-strands contains two lysines located very close to each other. It is very interesting to note that in DtX, DpI, and DpK the cationic amino acid residues at the N-terminal region are located in close proximity to those occurring at the β-turn, forming a positively charged cloud.

The overall conformation of the dendrotoxins does not differ much from the original structures derived from model building. The root mean square fluctuations of the C^{α} atoms of the three structures are shown in Figure 1. A careful analysis reveals that, in general, the fluctuations of the C^{α} atoms is greater in DpK than in DtX and DpI. It is mostly in the range 1−2 Å with a few exceptions. As in the case of BPTI,[18−20] the general trend observed in all the dendrotoxin structures is that the two strands of the β-sheet and the α-helix region have smaller fluctuations, while the regions around residues 9−13 and residues 25−28 (β-turn) have larger fluctuations.

The root mean square deviations of the backbone torsions ϕ and ψ are in the range 7−36°, 8−92°, and 9−43° for DpK, DtX, and DpI, respectively (refer to Figures 2). Larger fluctuations of ϕ and ψ are observed for the residues occurring near the C and N termini and in the turns between the β strands. In DtX and DpI, the region corresponding to the β-turn exhibits larger fluctuations. The mean fluctuation of the side chains of lysine residues is nearly 2 Å.

The region corresponding to high fluctuations of ϕ and ψ also corresponds to the regions of high fluctuations of bond length and angles. This suggests a rearrangement of the structures in these regions from the original structures obtained from that of BPTI. The time-averaged ϕ and ψ values of DtX, DpI, and DpK are deposited as Supporting Information (Table 7). The major secondary structural regions are conserved during the entire dynamics simulation. A comparative analysis of all the three dendrotoxins is given in Table 6.

Coordination of Waters around the Cationic Residues. Lysines have been shown to play an important role in neurotoxin binding to acetylcholine receptor. EPR and fluorescence studies, of both uncomplexed and complexed neurotoxins, provide evidence that the labels bind covalently to the ϵ-amino group of lysine residues and that these lysines might be exposed for binding by solvents or the anionic sites of the receptors. Any alteration of lysines and arginines significantly reduces the toxicity.[40] Due to the importance of lysines and arginines, the solvent coordination numbers of these residues were determined to gain an insight into understanding the binding interactions of these residues with the acetylcholine receptor.

Average solvent coordination number and distance were determined using the MDANAL module of AMBER.[28] The solvent coordination number of lysines is in general greater than that of arginines in the dendrotoxins. In DpK, the average coordination number, distances, and angles for lysines are in the range 2.1−3.5, 3.0 −3.04 Å, and 122.5−132.5°, respectively. The corresponding values for arginines are 0.2−2.99, 3.03−3.09 Å, and 70.2−121.2°, respectively. In DtX, the average coordination number, distances, and angles for lysines are in the range 1.8−4.06, 3.02−3.04 Å, and 127.2−131.7°, respectively. The corresponding values for arginines are 0.4−2.95, 3.0−3.1 Å, and 55.9−139.8°, respectively. The coordination number for lysine is greater than that for arginine with the mean ranging from 1.8 to 3.66 for lysines and from 1.2 to 2.8 for arginines.

Disulfide Bridges. The disulfides offer the maximum stability to the overall architecture of the dendrotoxins. Table 2 lists the conformational data of the disulfides observed in DtX, DpI, DpK, BPTI, and α-DtX (X-ray crystal structure[24]). The torsion angle χ_3 around the disulfide bond along with χ_2, $\chi_{2'}$ (for definitions of χ_2, χ_3, $\chi_{2'}$, see table legend) describes the conformation of the disulfide bridge (left-handed spiral, right-handed hook, etc.) In DtX, disulfide I (Cys 5-Cys 55) and disulfide III (Cys 14-Cys 38) correspond to a left-handed hook with a $C^{\alpha}\cdots C^{\alpha'}$ separation of 4.9 Å. Disulfide II occurs in a right-handed spiral conformation exhibiting *trans−gauche−trans* pattern for χ_2, χ_3, $\chi_{2'}$ with a long separation for $C^{\alpha}\cdots C^{\alpha'}$ (6.6 Å). In DpI, disulfide I occurs in left-handed spiral conformation with a $C^{\alpha}\cdots C^{\alpha'}$ distance of 5.3 Å, while disulfides II and III occur in right-handed hook conformation with $C^{\alpha}\cdots C^{\alpha'}$ separations of 5.1 and 6.3Å, respectively. In DpK, disulfide I has right-handed spiral conformation with $C^{\alpha}\cdots C^{\alpha'}$ distance equal to 5.1 Å while disulfide II and III occur in left-handed hook conformation (with $C^{\alpha}\cdots C^{\alpha'} = 5.0$Å for II and $C^{\alpha}\cdots C^{\alpha'} = 6.5$Å for III).

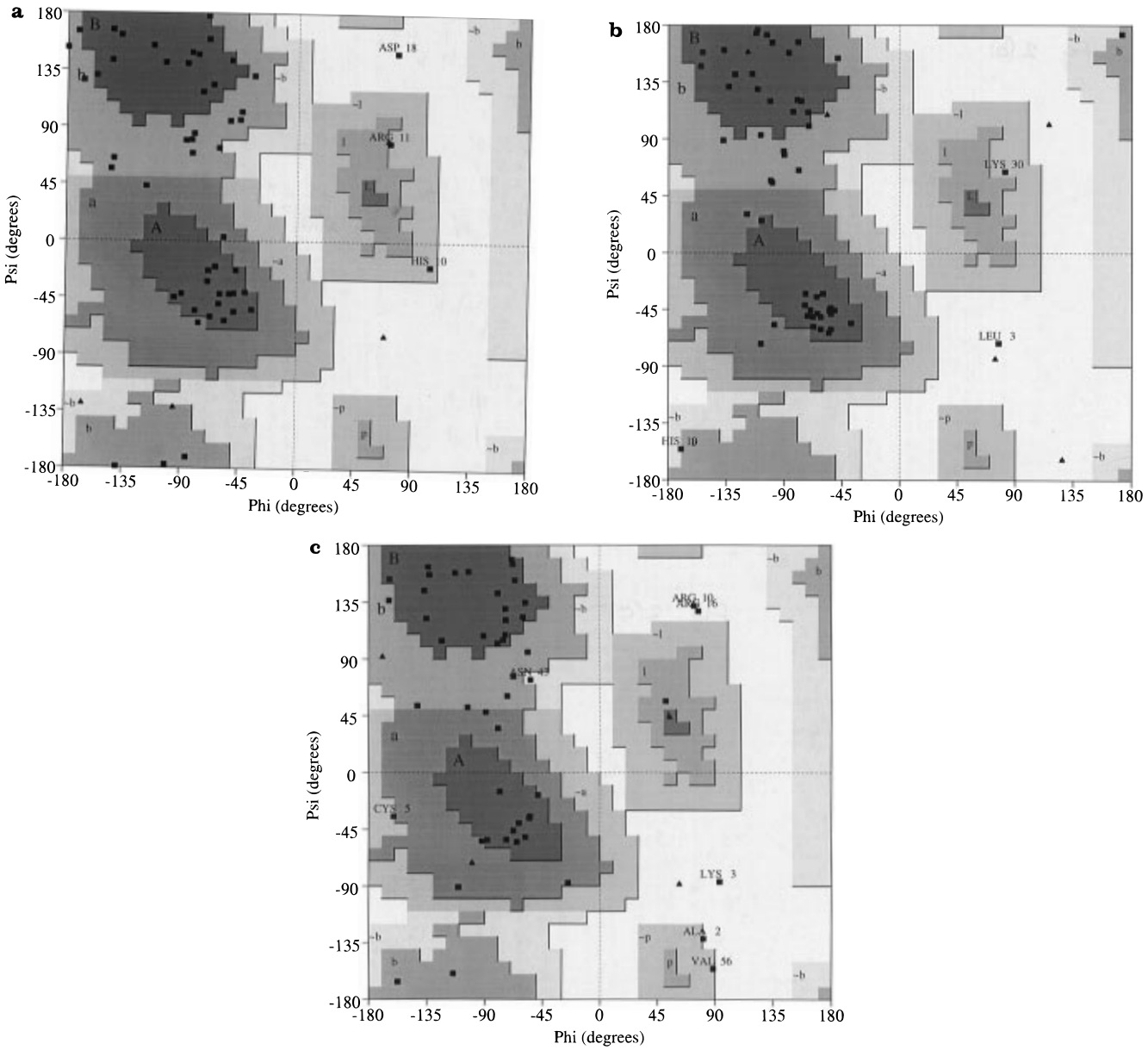

Figure 2. Ramachandran plot of the backbone torsion angles (ϕ, ψ) for (a) DtX, (b) DpI, and (c) DpK (computed using the program PROCHECK[59]). The shading represents the different regions of the plot; the darker the area the more favorable the region. Core regions are indicated by [A, B, L]; additional allowed regions by [a, b, l, p] and generously allowed regions by [~a, ~b, ~l, ~p]. Glycines are shown by solid triangles.

Disulfide I spans N- and C-terminal regions in the dendrotoxins and BPTI. In DtX, Cys 5 is part of a 3_{10} (short) helix while Cys 55 occurs at the end of an α-helix. In DpI, Cys 5 occurs in α-helical conformation while Cys 55 occurs at the end of α-helix. In DpK, Cys 5 occurs in an extended conformation while Cys 55 is at the end of the α-helix.

Disulfide II occurs between strands of amino acids which are continuations of the two antiparallel β-sheets in all the three structures. Due to geometrical reasons, a disulfide cannot be formed between the adjacent strands of β-sheets (parallel or antiparallel). However, a disulfide bridge is usually observed one or two residues out from the last hydrogen bond on one strand and three or four residues out on the other strand.[41] Occurrence of disulfide II in the present case belongs to this category.

Disulfide III spans the two major structural domains *viz.* the α-helix (at the C-terminus) and the antiparallel β-sheet, in all the three toxins (including BPTI). It is interesting to note that the $C^{\alpha}\cdots C^{\alpha'}$ distance for disulfide III is greater than 6.3 Å in all the structures reported in Table 2. Similar long disulfides have been reported in the structures of immunoglobulins where the disulfides spanning β-barrels have $C^{\alpha}\cdots C^{\alpha'}$ separations in the range of 6.6 to 7.4 Å. These long disulfides are *trans−gauche−trans* (±180°, ±90°, ±180°) in χ_2, χ_3, $\chi_{2'}$. A close look at the values of χ_2, χ_3, $\chi_{2'}$ reveals that they have *trans−gauche−trans* pattern for disulfide III in the toxins.

It is interesting to note that in DtX, DpI, and DpK the pentapeptide sequence Cys 51-x-x-x-Cys 55 at the carboxy terminus occurs in an α-helical conformation. The helix is stabilized by two disulfide bridges, one involving Cys 5 at the N-terminal and the other (Cys 30) at the β-strand. It has been reported that homologous cysteine distribution among neurotoxins is responsible for the occurrence of an ordered conformational motif consisting of an α-helix disulfide bonded to a β-strand, independent of the intervening amino acid sequence between the two cysteines,[42] which is in agreement with our observation in DtX, DpI and DpK.

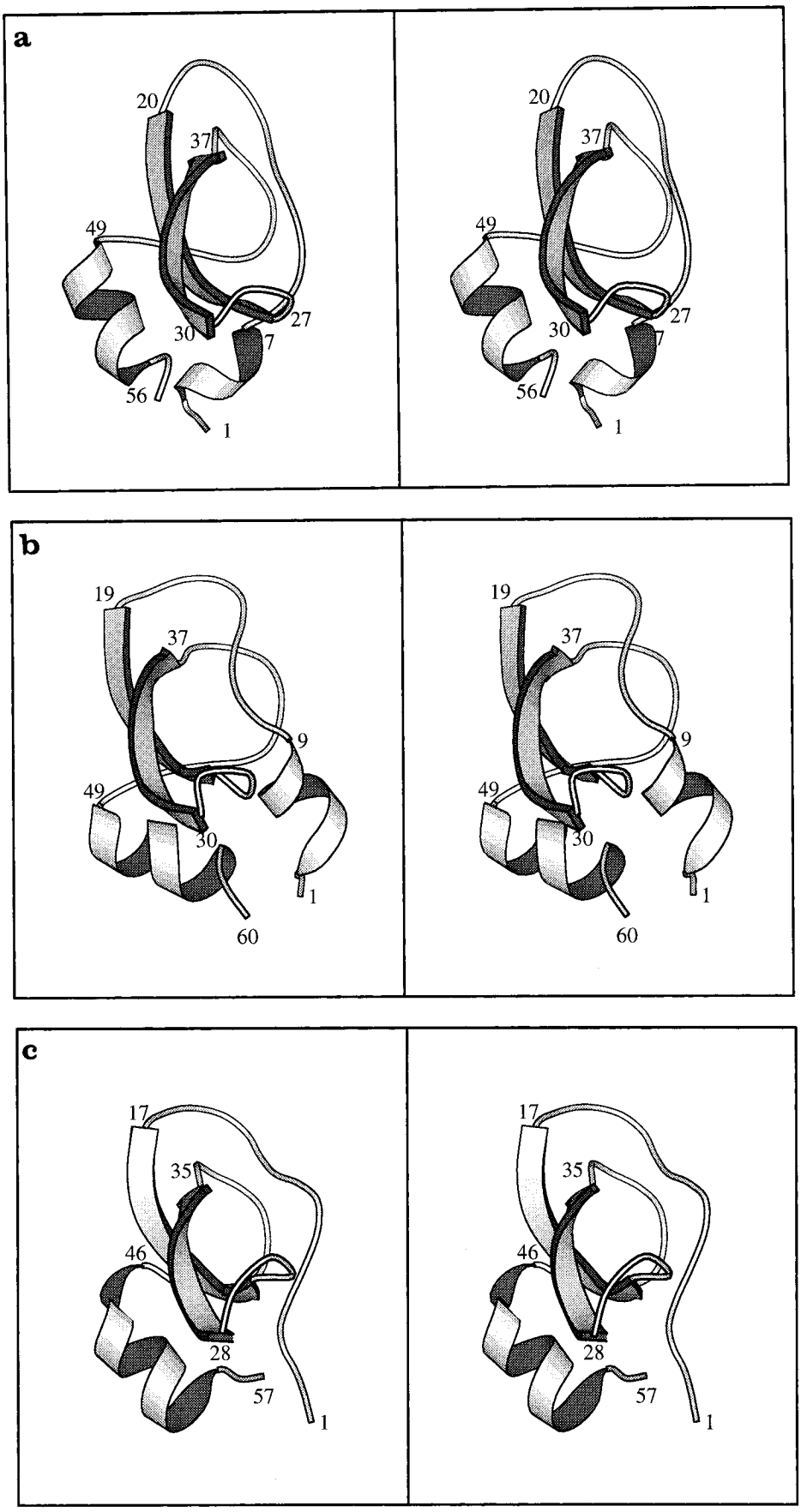

Figure 3. Schematic backbone drawings of (a) DtX, (b) DpI, and (c) DpK showing the secondary structure of the molecule (prepared using the program MOLSCRIPT[60]). The Arabic numerals stand for the beginning and end sequence number for the various secondary structural fragments.

It is important to note that the refolding pathway of DpI and DpK consists of the sequential formation of the three disulfides, first (Cys 30−Cys 51), then (Cys 5−Cys 55), and finally (Cys 14−Cys 38). The intermediate having the two disulfides (Cys 30−Cys 51) and (Cys 5−Cys 55) has been reported to have native like

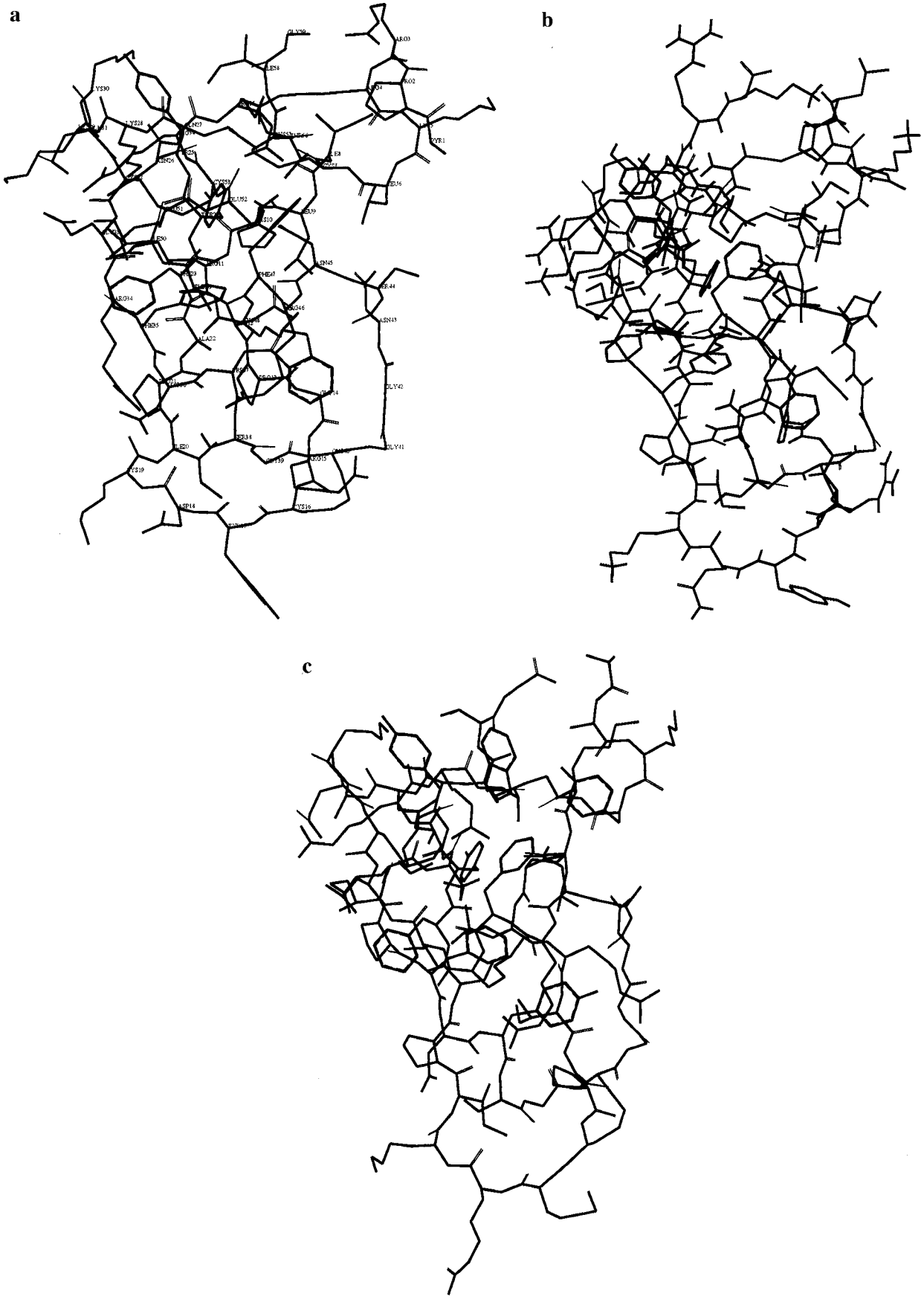

Figure 4. Wire frame diagram showing the non-hydrogens of the molecular structures of (a) DtX, (b) DpI, and (c) DpK.

conformation with significant K^+ channel binding activity.[46]

Hydrogen Bond Interactions. The three-dimensional structure and the folding of the three dendrotoxins are mainly stabilized by the three disulfides as described in the previous sections. In addition, there are several intramolecular hydrogen bonds, which offer additional stability to the secondary structural regions of the toxins. Interhelical interactions are mostly due to disulfides and intramolecular hydrogen bonds. The

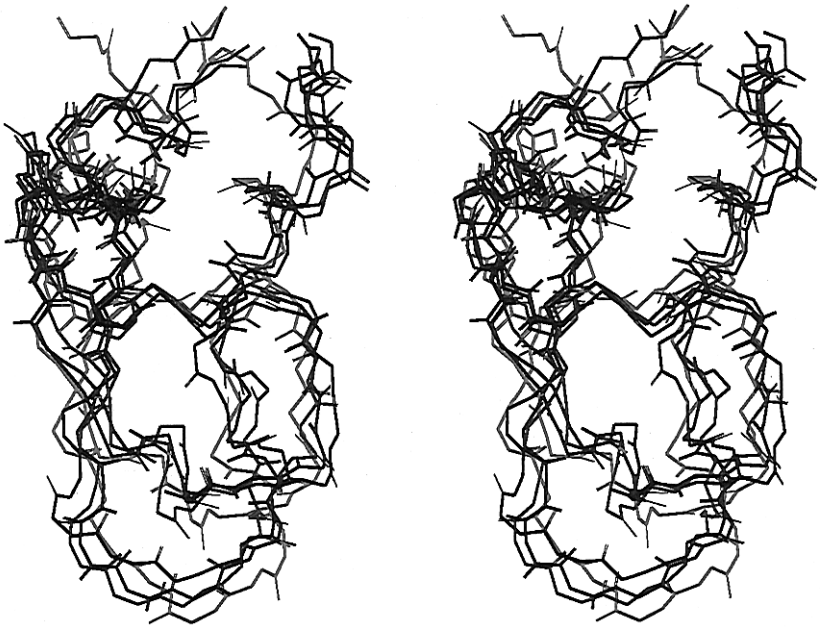

Figure 5. Stereoview of the superposition of the backbone atoms of DtX, DpI (in blue), DpK (in green), and crystal structure of α-dendrotoxin (in red). The rms differences between the toxins are listed in Table 6.

Table 2. Disulfide Geometry and Conformational Characteristics

molecule	disulfide[a]	χ_1[b] (deg)	χ_2[b] (deg)	χ[b] (deg)	χ'_2[b] (deg)	χ'_1[b] (deg)	$C^\alpha \cdots C^{\alpha'}$ (Å)
DtX	I	−136	−163	−85	100	−168	5.21
DpI	I	−54	−45	−91	−44	−94	5.05
DpK	I	−145	142	−80	119	114	4.93
BPTI	I	−72	−66	−83	−61	−74	5.46
α-DtX (cryst)	I	−66	−77	−87	−65	−63	5.21
DtX	II	−75	177	−106	43	26	4.95
DpI	II	−77	82	98	−107	85	5.20
DpK	II	−58	178	−106	157	82	5.00
BPTI	II	−74	96	97	−118	69	5.50
α-DtX (cryst)	II	−79	93	91	−107	−71	4.95
DtX	III	−178	173	−94	153	49	6.18
DpI	III	−178	99	98	−166	−172	6.15
DpK	III	152	−141	−99	157	82	6.50
BPTI	III	−72	−121	−81	−97	−179	6.27
α-DtX (cryst)	III	−68	−101	−88	−88	177	6.26

[a] I, Cys 5-Cys 55; II, Cys 16-Cys 38; III, Cys 30-Cys 51. [b] χ_1, χ_2, χ_3, χ'_2, and χ'_1 are defined as follows:

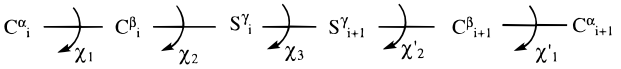

time-averaged hydrogen bond distances (reported in Tables 3−5) were calculated from the trajectories of the molecular dynamics simulations computed between 100 and 200 ps, using the MDANAL module of AMBER.[28]

There are 49 intramolecular hydrogen bonds observed in the structure of DtX. It is interesting to note that Arg 2 at the N-terminus is involved in hydrogen bond interaction (formed during the MD simulation) to Gly 57 at the C-terminus as well as to Cys 5 (part of 3_{10} helix). In addition, Leu 9 (helix terminal residue) is hydrogen bonded to Asn 43, and Gly 25 (occurring at the β-turn). Similarly, Cys 5 is hydrogen bonded to Gly 25, offering additional stability to the β-turn and the 3_{10} helix. The carbonyl oxygen of Ser 36 is hydrogen bonded to Arg 13 (NH) and Cys 38 (NH). The hydroxyl oxygen O^γ of Ser 36 is located at a distance of 2.18 Å from Cys 38 (O), suggesting a possible hydrogen bond interaction. The antiparallel β-strands are stabilized by three intramolecular hydrogen bonds. These are further stabilized by the hydrogen bond interactions between Ile 18, Pro 19, and Arg 44. The β-turn residues are involved in a network of hydrogen bonds involving Asn 24···Lys 28, Lys 27···Glu 31, and Asn 24···Glu 31. The α-helix at the C-terminus is stabilized by five hydrogen bonds. DtX contains 14 positively charged amino acid residues and 5 negatively charged residues. Of these, four positively charged residues form salt bridges with four negatively charged residues, *viz*. Lys 27···Glu 31, Asp 34···Arg 32, Glu 50···Arg 53, and Glu 49···Arg 52.

Out of the 39 intramolecular hydrogen bonds observed in DpI, three stabilize the α-helix at the N-terminus, seven occur between the two antiparallel β-strands, and six occur in the α-helical region at the C-terminus. The β-turn takes part in five hydrogen bonds. The hydrogen-bonding interactions between the residues Pro 11···Ser 36 and Phe 21···Phe 45 offer additional stability for the β-strands. O^γ of Ser 36 is involved in hydrogen bonding with carbonyl O of Gly 12. There are two salt bridges observed between Lys 27···Glu 31 and Glu 50···Arg 53.

DpK structure is stabilized by a total of 26 hydrogen bonds. The two antiparallel β-strands exhibit four hydrogen bonds involving the carbonyl oxygens and amide nitrogens. Additional stability of the β-strands

Table 3. Average[a] Hydrogen Bond Distances Observed in DtX

donor (D)	acceptor (A)	distance Å
Arg 2 NH	O2 Gly 57	2.24
Arg 2 $N^{\epsilon}H$	O2 Gly 57	2.16
Cys 5 NH	O Arg 2	2.17
Leu 7 NH	O Leu 4	2.21
Gln 25 $N^{\epsilon 1}H$	O Cys 5	1.94
Gln 25 $N^{\epsilon 2}H$	O Leu 7	2.16
Arg 13 NH	O Ser 36	2.21
Cys 14 NH	O Ser 36	2.29
Arg 44 $N^{\eta 1}H_2$	O Ile 18	1.90
Arg 44 $N^{\eta 2}H_2$	O Pro 19	2.17
Phe 33 NH	O Ala 20	2.32
Phe 21 NH	O Phe 45	2.00
Tyr 22 NH	O Glu 31	1.99
Glu 31 NH	O Tyr 22	2.13
Asn 24 NH	O Gln 29	1.92
Lys 26 NH	$O^{\delta 1}$ Asn 24	2.26
Lys 27 NH	$O^{\delta 1}$ Asn 24	2.02
Asn 24 $N^{\delta 1}H$	$O^{\epsilon 1}$ Glu 31	2.11
Lys 28 NH	O Asn 24	2.37
Lys 27 $N^{\zeta 2}H$	$O^{\epsilon 2}$ Glu 31	2.27
Arg 44 $N^{\eta 1}H_1$	O Trp 35	1.93
Trp 35 $N^{\epsilon}H$	O Asn 43	2.23
Cys 38 O	O^{γ} Ser 36	2.18
Asn 43 NH	$O^{\delta 1}$ Asn 41	2.06
Arg 44 NH	O Ser 42	2.15
Cys 51 NH	$O^{\epsilon 2}$ Thr 47	2.00
Arg 52 NH	O Ile 48	1.94
Arg 52 $N^{\eta 1}H_1$	$O^{\epsilon 2}$ Glu 49	1.93
Arg 53 NH	O Glu 49	2.47
Arg 53 $N^{\eta 2}H_2$	$O^{\epsilon 1}$ Glu 50	1.86
Arg 53 $N^{\eta 1}H_2$	$O^{\epsilon 2}$Glu 50	1.77
Thr 54 NH	O Glu 50	2.31
Thr 54 $O^{\gamma}H$	O Glu 50	2.33
Cys 55 NH	O Cys 51	2.14

[a] Atom names of the amino acids are based on IUPAC nomenclature.[58] The sequence numbering is based on the BPTI structure.

Table 4. Average[a] Hydrogen Bond Distances Observed in DpI

donor (D)	acceptor (A)	distance Å
Arg 2 NH	O Pro 0	2.27
Cys 5 NH	O Arg 2	2.16
Ile 6 NH	O Arg 2	2.33
Ile 6 NH	O Lys 3	2.36
Leu 7 NH	O Lys 3	2.32
Arg 9 $N^{\eta 2}H_1$	O Gly 32	2.16
Gly 12 NH	$O^{\delta 1}$ Asn 10	2.19
Ser 36 NH	O Pro 11	1.95
Ser 36 $O^{\gamma}H$	O Gly 12	2.39
Cys 14 NH	O Cys 38	2.47
Ile 18 NH	O Trp 35	2.17
Trp 35 NH	O Ile 18	1.96
Ala 20 NH	O Phe 33	2.20
Phe 33 NH	O Ala 20	1.96
Phe 21 NH	O Phe 45	1.99
Arg 44 NH	O Phe 21	1.89
Tyr 22 NH	O Glu 31	2.02
Tyr 22 $O^{\gamma}H$	O Glu 31	1.80
Glu 28 NH	O Tyr 22	1.93
Tyr 23 NH	$O^{\delta 1}$ Asn 43	2.02
Arg 44 NH	O Asn 41	2.23
Asn 43 $N^{\delta 2}H$	O Tyr 23	1.96
Asn 24 NH	O Gln 29	1.93
Lys 26 NH	$O^{\delta 1}$ Asn 24	2.43
Lys 27 NH	$O^{\delta 1}$ Asn 24	2.03
Asn 24 $N^{\delta 1}H$	$O^{\epsilon 1}$ Glu 31	2.39
Lys 28 NH	O Asn 24	2.24
Gln 29 NH	O Asn 24	2.17
Trp 35 $N^{\epsilon}H$	O Gly 39	2.07
Cys 51 NH	O Thr 47	2.10
Arg 52 NH	O Ile 48	2.04
Arg 52 $N^{\eta 2}H_1$	$O^{\epsilon 2}$ Glu 49	2.02
Arg 53 NH	$O^{\epsilon 1}$ Glu 49	2.44
Arg 53 $N^{\epsilon}H$	$O^{\epsilon 1}$ Glu 50	2.21
Arg 53 $N^{\eta 2}H_1$	$O^{\epsilon 1}$ Glu 50	2.39
Arg 53 $N^{\eta 2}H_1$	$O^{\epsilon 2}$ Glu 50	2.41
Thr 54 NH	O Glu 50	2.06
Cys 55 NH	O Cys 51	2.31

[a] Atom names of the amino acids are based on IUPAC nomenclature.[58] The sequence numbering is based on the BPTI structure.

is provided by the hydrogen-bonding interactions between Ser 20···Arg 44 and Phe 21···Phe 45. The α-helix at the C-terminus is stabilized by four hydrogen bonds parallel to the helix axis. In addition, there is a salt bridge between Glu 49 and Arg 53.

A comparison of the hydrogen-bonding patterns observed in the three toxins reveals that the two antiparallel β-strands are further stabilized by hydrogen-bonding interactions between the amino acids at positions 11−13 and 36−38 at one end and between residues at locations 24−26 and 43−45 at the other end. The hydrogen-bonding pattern involving Ser 36 residue is similar in DtX, DpI, and the crystal structure of α-DtX.[24] It has been reported[16] that Ser 36 could disrupt the inhibitory activities of the dendrotoxins by competing with Ser 195 of trypsin for hydrogen-bonding to the catalytic residue His 57. Our observation suggests that the intramolecular hydrogen bonding interactions between Ser 36 and the neighboring residues of DtX and DpI are more favorable and thus may prevent Ser 36 from hydrogen bonding with His 57 of trypsin.

Interactions between the Dendrotoxins and the Proteinases. A sample view of the residues at the anti-protease site of DtX in complex with kallikrein and trypsin is given in Figures 6 and 7. Figures 8 and 9 show a stereoview of the C^{α} plots of the dendrotoxins in complex (built by comparative modeling) with trypsin and kallikrein. Residues 13−20 of DtX and DpI correspond to the anti-protease site of BPTI which binds to trypsin and kallikrein. Out of these eight residues, only three residues, *viz*. Gly14, Cys16, and Ile 20, are common between the DtX, DpI, and BPTI. The details of the nonbonded interactions involving the dendrotoxins and trypsin and kallikrein residues at the anti-protease site are submitted as Supporting Information (Tables 8 and 9).

Dendrotoxins and Kallikrein. The p1 residues Tyr 15 (DtX, DpI) and Lys 15 (DpK) make numerous nonbonded contacts with the residues of kallikrein. The aromatic ring of Tyr 15 is sandwiched between Trp 215 and Asp 194 of kallikrein. There are five nonbonded contacts between Lys 15 (DpK) and the residues of kallikrein which are different from those observed in the BPTI−kallikrein complex.[37] The torsion angle χ_1 ($N-C^{\alpha}-C^{\beta}-O^{\gamma}$) of Ser 195 is in the range −59 to −110° in all three complexes. The p2 residue (Cys 14) of DtX and DpI is not involved in any significant nonbonded interaction with the residues of kallikrein, while p3 residue Arg 13 (DtX, DpI) is involved in four nonbonded contacts with the residues of kallikrein. The orientation of Tyr 99 is perpendicular to the indole ring of Trp 215 (kallikrein). It has been reported that Tyr 99 (kallikrein) swings its position to accommodate the presence of bulky Cys and Arg residues at the p2 and p3 positions in the BPTI−kallikrein complex.[37] The p3 residue (Pro 13) of DpK is not involved in any significant nonbonded interaction with the residues of kallikrein. The p1′ and p2′ residues of DtX, DpI, and DpK make numerous nonbonded contacts with the residues of kallikrein. It is important to note that the p1′ residues Asp 16 (DtX), Gln 16 (DpI), and Arg 16 (DpK) are involved in significant nonbonded interactions with the Ser 195 (*catalytic*) residue of kallikrein. The number of non-

Table 5. Average[a] Hydrogen Bond Distances Observed in DpK

donor (D)	acceptor (A)	distance Å
Tyr 4 NH	O Ala 2	2.46
Leu 7 NH	O Cys 5	2.16
Cys 14 NH	O Ser 36	2.24
Ile 18 NH	$O^{\delta 1}$ Asp 34	2.17
Ser 20 NH	O Phe 33	2.01
Arg 44 $N^{\eta 2}H_1$	O^{γ} Ser 20	1.86
Phe 33 NH	O Ser 20	1.92
Phe 21 NH	O Phe 45	2.00
Tyr 22 NH	O Leu 31	2.30
Leu 31 NH	O Tyr 22	1.98
Lys 24 NH	O Gln 29	2.51
Ala 27 NH	O Trp 25	2.37
Gln 29 $N^{\epsilon 1}H$	O Cys 30	2.46
Asn 41 NH	O^{γ} Tyr 35	2.10
Tyr 35 $O^{\gamma}H$	O Asn 41	1.99
Gly 37 NH	O Tyr 35	1.96
Cys 38 NH	O Ser 36	1.95
Ala 42 NH	$O^{\delta 1}$ Asn 41	2.32
Arg 44 NH	O Ala 42	2.05
Thr 47 NH	O Phe 45	2.06
Thr 47 $O^{\gamma}H$	O Lys 46	2.20
Glu 50 NH	O Thr 47	2.15
Arg 52 NH	O Ile 48	2.06
Arg 52 $N^{\epsilon}H$	$O^{\epsilon 2}$ Glu 49	2.00
Arg 53 NH	O Glu 49	2.33
Arg 53 $N^{\eta 1}H_2$	$O^{\epsilon 1}$ Glu 50	2.02
Arg 53 $N^{\eta 2}H_2$	$O^{\epsilon 2}$ Glu 50	2.11
Thr 54 NH	O Glu 50	2.01
Cys 55 NH	O Glu 50	2.09

[a] Atom names of the amino acids are based on IUPAC nomenclature.[58] The sequence numbering is based on the BPTI structure.

Table 6. Comparative Analysis of the Dendrotoxins[a]

α-DtX (xtal)	0.0	2.59	2.23	2.30
DtX	59 (100%)	0.0	1.36	1.03
DpK	37 (62%)	37 (62%)	0.0	1.17
DpI	55 (93%)	55 (93%)	36 (61%)	0.0

[a] The values in the lower triangular part of the matrix give the number of residues common between the proteins with the percentage of homology given in parentheses. The values in the upper triangular part of the matrix gives the rms difference between the proteins (computed using the backbone atoms).

bonded contacts between p1′ site and kallikrein is greater than that of the corresponding ones between the p1 site and kallikrein. The number and nature of interactions involving the p2′ site (lysine in all the three dendrotoxins) is different from those observed in the BPTI−kallikrein complex.[37]

Dendrotoxins and Trypsin. The nonbonded interactions between p1 residue Tyr 15 (DtX, DpI) and residues of trypsin are very similar to those observed in the kallikrein complex. The torsion angle χ_1 ($N-C^{\alpha}-C^{\beta}-O^{\gamma}$) of Ser 195 (trypsin) is in the range −90 to −120°. Lys 15 (DpK) makes eight nonbonded contacts with the residues of trypsin. The nonbonded contacts involving p2 and p3 residues of DtX and DpI and the residues of trypsin are different from those reported for BPTI−trypsin complex.[36] As observed in the kallikrein case, the number of nonbonded interactions involving p1′ and p2′ sites and the residues of trypsin are greater than those involving the p1 residue. Similarly, the p1′ residue of the dendrotoxins take part in significant van der Waals interactions with trypsin Ser 195 residue as in the kallikrein case. The p2′ residue (of DtX and DpI) take part in two contacts with the residues of trypsin while in DpK the p2′ site is involved in seven nonbonded contacts with the residues of trypsin.

Comparison of Complexes: (a) Anti-Protease Site. The interactions involving the backbone atoms

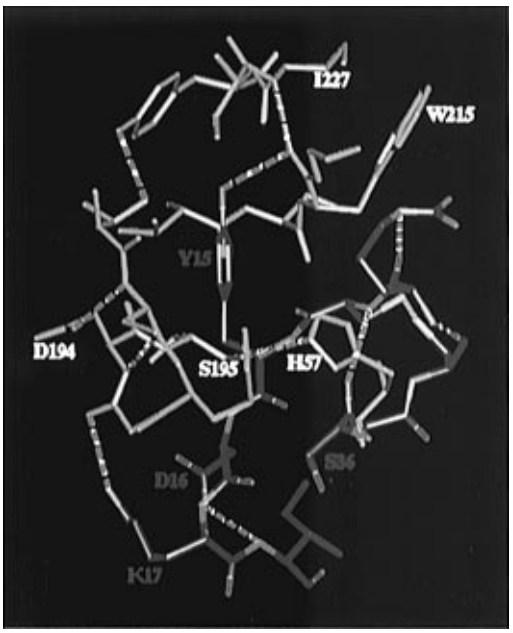

Figure 6. Surrounding of the anti-protease region of DtX in complex with kallikrein. Residues of DtX are shown in green and red, while those of kallikrein are shown in orange. Key hydrogen bond interactions are shown in dashed line (magenta). The distance between the hydroxyl of Ser 36 (DtX) and kallikrein His 57 is greater than 7.5 Å.

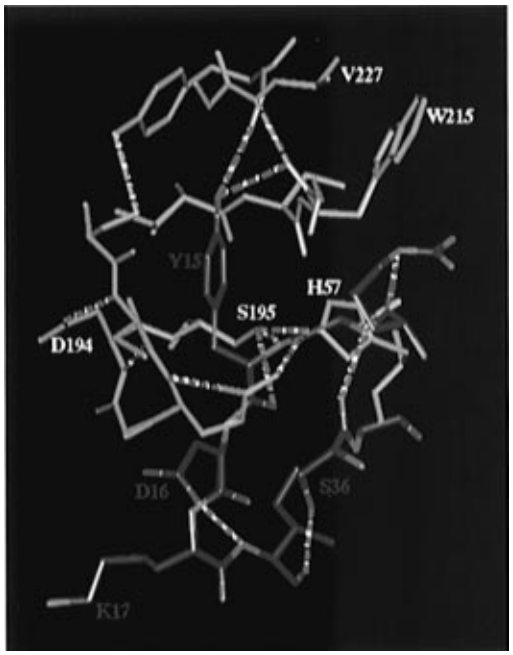

Figure 7. Surrounding of the anti-protease region of DtX in complex with trypsin. Residues of DtX are shown in green and red, while those of trypsin are shown in orange. Key hydrogen bond interactions are shown in dashed line (magenta). The distance between the hydroxyl of Ser 36 (DtX) and trypsin His 57 is greater than 7.5 Å.

of the *anti-protease* site of the dendrotoxins and trypsin and kallikrein structures are similar to those observed in the BPTI complex structures.[36,37] However, the side chain interactions of the *anti-protease* site of the dendrotoxins are different from those reported for BPTI due to differences in the amino acid sequence, at the anti-protease site, between BPTI and the dendrotoxins. The active site residue Lys 15 of BPTI is replaced by Tyr 15 in DtX and DpI. This has resulted in the disappearance of the key interaction between Lys 15 and Asp 189 (salt bridge) reported in the complex between trypsin and

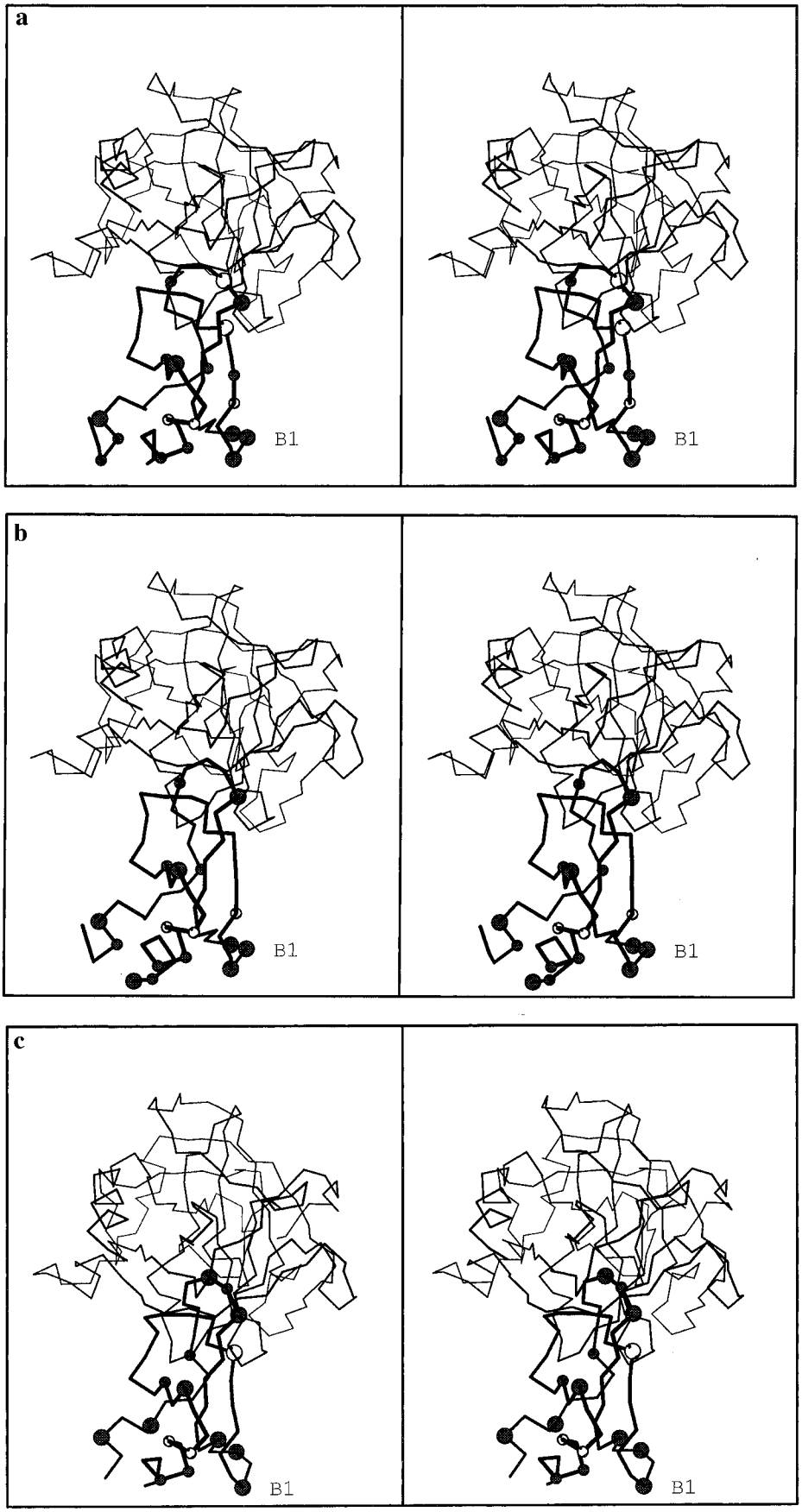

Figure 8. C^{α} plot of the model complex: (a) kallikrein−DtX, (b) kallikrein−DpI, and (c) kallikrein−DpK. Kallikrein is shown by thin lines, and the dendrotoxins by thick lines. The lysines (of toxins) are shown by solid spheres, and the arginines (of toxins) by open spheres. The proposed binding region of the dendrotoxins is shown by B1 (prepared using MOLSCRIPT[60]).

BPTI[36] and a similar interaction between Lys 15 and Asp 189 through a water molecule in kallikrein complex.[37] Instead, the hydroxyl of Tyr 15 is hydrogen bonded to Trp 215 and Thr 190 (of kallikrein) and Trp 215 and Ser 190 (of trypsin). The residues at the p1′ site are Asp 16 (DtX), Gln 16 (DpI), and Arg 16 (DpK).

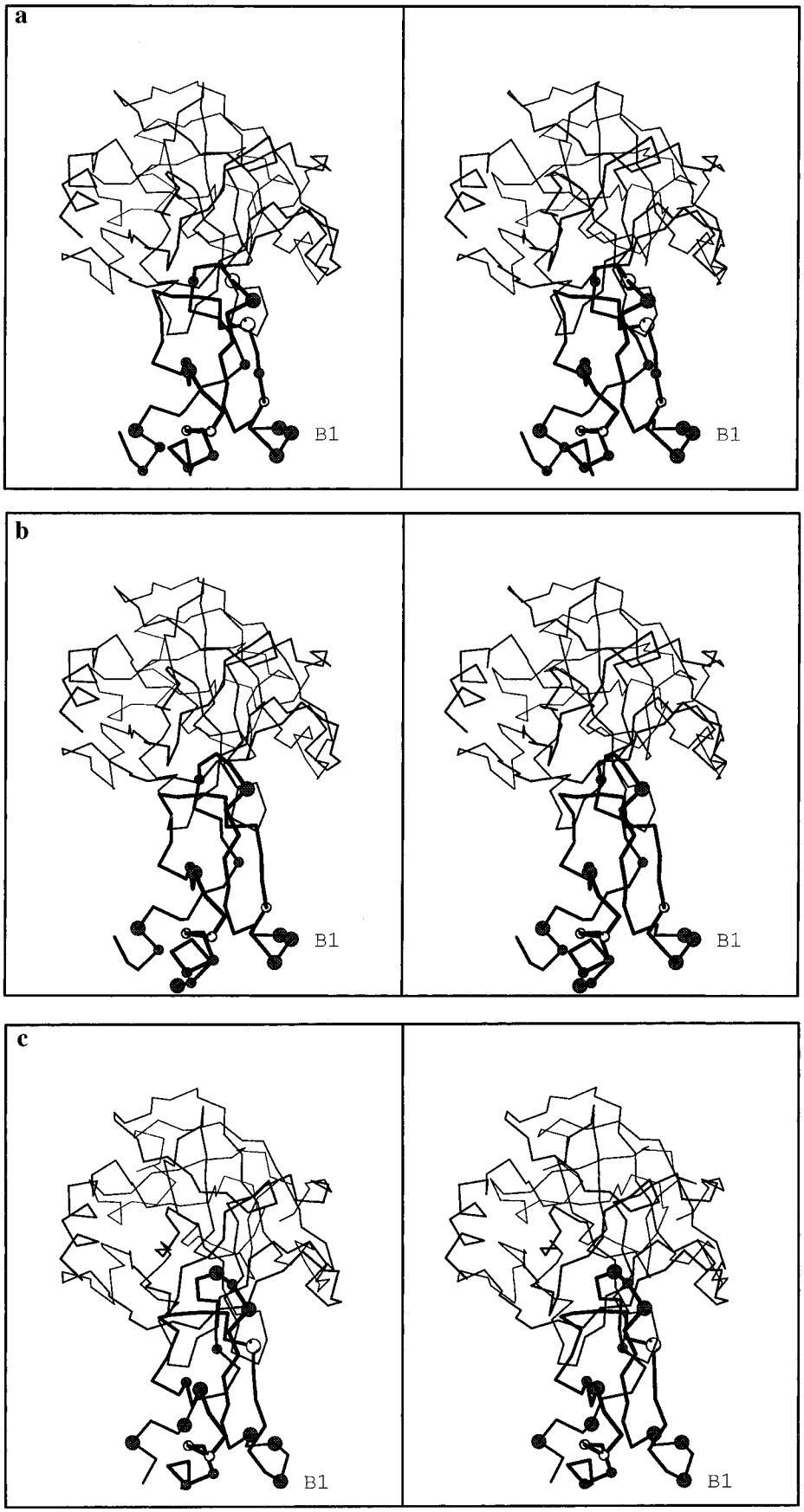

Figure 9. C^{α} plot of the model complex: (a) trypsin−DtX, (b) trypsin−DpI, and (c) trypsin−DpK. Trypsin is shown by thin lines, and the dendrotoxins by thick lines. The lysines (of toxins) are shown by solid spheres, and the arginines (of toxins) by open spheres. The proposed binding region of the dendrotoxins is indicated by B1 (prepared using MOLSCRIPT[60]).

In all of the protease inhibitors known so far, this site is occupied by either glycine or alanine. In addition, Lys 17 at the p2′ site is invariant in the dendrotoxins structures (the equivalent site is occupied by Arg 17 in BPTI). The absence of lysine at the p1 site and the presence of Lys 17 at the p2′ site along with the

occurrence of hydrophilic charged residues at the p1′ site (of the dendrotoxins) can rearrange the atom positions surrounding the junction region between the toxins and the proteinases (trypsin, kallikrein, etc.) and thus hinder the key interactions needed for protease activity. These differences in the intermolecular interactions between the dendrotoxins and the proteinases may explain the lack of anti-protease activity exhibited by the dendrotoxins, even though they are homologous to other proteinase inhibitors. However, this region (called anti-protease site) does not seem to explain the potassium channel blocking properties of the dendrotoxins. This feature is discussed in the following section.

(b) Region of Cationic Amino Acid Residues. Dendrotoxins enhance the release of neurotransmitters at the motor nerve terminals by specifically blocking the voltage sensitive potassium channels.[43,44] Comparison of the amino acid sequences of DtX, DpI, and DpK shows that the five amino acids at positions 3, 17, 19, 26, and 28 (based on BPTI numbering) are identical, with four of them as lysines. In addition, in the structures of DtX and DpI, three of the lysines (Lys 26, 27, and 28) occur (in a cluster) contiguously which is unusual. In DpK, the residues 26 and 28 are lysines and residue 27 is alanine. In β-bungarotoxin the corresponding residues are arginine, leucine, and lysine (Table 1). Thus there is a sufficient concentration of positive charges in a narrow region (β-turn) exposed to the surface of the dendrotoxins. Even in the complexed model structures, this region is clearly exposed for binding by anionic sites of the receptors (refer site B1 in Figures 8 and 9). It has been reported[4,45] that the presence of three contiguous lysine residues results in a cluster of positive charges in a narrow region of the protein and thus a possible binding region of the dendrotoxins to their target site. Using partially folded versions of DpI and DpK from black mamba (by selectively reducing the disulfide bridges), Hollecker and co-workers[46] reported that the regions containing the two disulfide bridges around (Cys 5−Cys 55) and (Cys 30−Cys 51) and the lysine residues located at the base of the toxins are important for the activity of the dendrotoxins. The lysines may take part in an ionic interaction with the negatively charged residues on the surface of the K^+ channels.

Using recombinant DNA techniques, Hurst and co-workers[47] have cloned DtX sensitive rat potassium channels. Their studies have revealed that the negatively charged amino acid residues at the *trans* membrane loop (pore forming sequence)[48] between the regions S5−S6 are important for the binding of the dendrotoxins. Specifically, the negatively charged K^+ channel residues Glu 353 and Tyr 379 are critical for the blocking of K^+ channel by DtX, and alteration of these residues to serine or histidine significantly lowers the affinity of DtX in blocking the potassium channels. Cation selective channels in general, and potassium channels in particular, are thought to have a permeation pathway preceded by a cloud of negative charges, which contribute to ion selectivity and ion permeability.[49] Yool and Schwartz[50] have reported that by selectively changing two amino acids, the ion permeability of the channels can be significantly altered without altering the structure of the pore region. The two amino acids, carrying a negative charge located at the mouth of the pore region, influence the binding of the TEA (tetraethylammonium), DtX, etc. These amino acids do not alter the ion selectivity, but block the entrance of the ions into the channel. The importance of the charge, basicity, and geometrical positions of the cationic amino acids in the activity of μ-conotoxin has been reported by Sato and co-workers.[51] These observations indicate that, in the case of the dendrotoxins, the geometrical locations of the cationic amino acids carrying the positive charges (lysines and arginines) may give us an insight into understanding their structure−activity relationships.

As is evident (from site B1 in Figures 8 and 9), the invariant contiguous lysines at positions 26, 27, and 28 are exposed to the surface and thus facilitate binding by the anionic sites of K^+ channel. In the case of DpK, the two lysines (intervened by alanine) are exposed to the surface. It is important to note that these exposed lysines occur at the hairpin turns bridging two antiparallel β-sheets in all three toxins. It is well established that hairpin turns and bends occur very frequently in protein structures and that they play a crucial role in protein folding.[52] The geometrical positions and the mobility of the side chains of lysines indicate that these can make potential interaction with the anionic sites (negatively charged amino acid residues) located at the mouth of the pore region extracellular to the channel membrane. This can lead to blocking of the channel by the dendrotoxins by direct binding. On the basis of experiments with excised and cell attached recording, it has been reported that Tityustoxin-Kα (TsTX-Kα) (a channel peptide toxin) and α-DtX block the K^+ channel by binding to the same or closely related extracellular site.[53] In contrast, the binding of 4-aminopyridine was not inhibited by α-DtX or TsTx-Kα in the same experiment, suggesting that the mode of action of 4-aminopyridine is different from that of α-DtX. Our model supports the finding that α-DtX blocks the channel by binding extracellularly at the pore region. In the structural analysis of Conotoxin GIIIA in aqueous solution, it was observed that the seven cationic side chains of lysines and arginines project radially into the solvent and form potential sites for binding with the skeletal muscle sodium channel.[54] The greater mobility of the side chains of these cationic residues was interpreted as useful for a good fit to a receptor by local optimized interactions of those side chains. That the lysine residues (26−28) remain exposed even in the complexed form reiterates the fact that these lysines might act as a binding site for the anionic residues of the receptors.

The degree of sequence homology between the dendrotoxins and their inactive counter parts (most of them proteinase inhibitors) is maximum at the C-terminal half (residues 32−60) and minimum at the N-terminal half of the dendrotoxins (residues 1−31).[55] Based on homology, it has been reported that the N-terminal portion of the toxins contributes to the neurotoxicity of the toxins.[55] It is interesting to note that all the invariant lysines observed in the sequence of the dendrotoxins occur at the N-terminal half, consistent with the previous observation.

Disulfides play a crucial role in determining the rate and nature of protein folding. The strikingly homologous distribution of cysteines in DtX, DpI, and DpK seems to influence the homologous folding of the den-

drotoxins with the occurrence of a characteristic conformational pattern consisting of an α-helix (in an amphiphilic environment at the C-terminus) stabilized by two disulfides, one bridging a β-strand and the other N-terminus. A similar conformational motif has been reported in the case of MCD peptide, apamin, charybdotoxin, etc.,[42] even though there is no significant sequence homology among these peptides and the dendrotoxins. Neurotransmitters, peptide toxins, hormones, etc. (membrane surface-active peptides with low molecular weight) fold into the bioactive state with the formation of ordered amphiphilic secondary structural fragments like α-helix and β-strands and turns in amphiphilic environments. These amphiphilic secondary structures provide the rigid framework needed for the steric display of the functional groups that interact with the corresponding template of the receptors.[56] It appears therefore that the occurrence of such a conformational motif in the dendrotoxins can be correlated to their ion channel function, as reported in the case of MCD peptide.[42] This is in agreement with the report (in the case of DpI and DpK) that the two disulfides Cys 30−Cys 51 and Cys 5−Cys 55 are critical for the overall stability and the binding affinity of the dendrotoxins.[46] The formation of these two disulfides, during the refolding of the dendrotoxins, induces the occurrence of the α-helix in an amphiphilic environment and thus provides a rigid framework needed for bringing together the critical cationic amino acids in close proximity to the surface of the toxins for binding by the anionic sites of the receptors. As a result, there is a concentration of positively charged amino acids in this region exposed to the receptors. Dendrotoxins inhibit the binding of MCD peptide at the hippocampal region.[57] It appears that MCD peptide, dendrotoxins, and β-bungarotoxin all bind to the same ancestral voltage sensitive potassium channel.[57] It has been reported that homologous spatial charge distribution may account for the similarities in activities of DtX, DpI, DpK, and MCD peptides,[25] which is in agreement with our observation. The presence of amphiphilic secondary structural fragments in the dendrotoxins and MCD peptide appears to induce the homologous spatial charge distribution among DtX, DpI, DpK, and MCD peptides.

Our analysis of DtX, DpI, and DpK reveals that their three-dimensional architectures and folding are similar to BPTI (the Kunitz proteinase inhibitor). The absence of anti-protease activity of the dendrotoxins can be attributed to the differences in the sequence and structure at the anti-protease site between BPTI and the dendrotoxins. The comparative model building studies, involving the dendrotoxins and proteinases, indicate that the proposed ion channel binding region of DtX, DpI, and DpK is the β-turn containing (cationic) residues 26−28 (site B1 of Figures 8 and 9) located roughly 25 Å from the anti-protease site, at the opposite side, of the pear-shaped molecules. Structural similarity between DtX, DpI, DpK, β-bungarotoxin, and MCD peptide suggests that these peptides regulate K^+ channel by direct binding to the extracellular trans-membrane loop spanning the (S5,S6) region.

Acknowledgment. P.S. wishes to express his sincere thanks to Drs. Leslie J. Humber and Ronald J. McCaully for their support and encouragement during the course of this work. The author also would like to thank Dr. Reinhardt Stein for many useful discussions and help in making the figures and Dr. A. R. Srinivasan for many invaluable comments. Our thanks are due also to the personnel of the supercomputer facility at Scripps Clinic and Research Foundation for helping one of us (M.H.) to run the AMBER program on their CRAY-YMP supercomputer.

Supporting Information Available: Time-averaged conformational (ϕ, ψ) angles of the dendrotoxins (Table 7) and nonbonded contacts between kallikrein and the dendrotoxins (Table 8) and between trypsin and the dendrotoxins (Table 9) (8 pages). Ordering information is given on any current masthead page.

References

(1) Harvey, A. L.; Karlson, E. Dendrotoxin from the Venom of the Green Mamba *Dendroaspis Angusticeps*. A Neurotoxin that Enhances Acetylcholine Release at Neuromuscular Junctions. *Naunyn-Schmiedebergs Arch. Pharmacol.* **1980**, *312*, 1−6.
(2) Joubart, F. J.; Taljaard, N. The Amino Acid Sequence of Two Proteinase Inhibitor Homologues from Dendroaspis Angusticeps Venom. *Hoppe-Seylers Z. Physiol. Chem.* **1980**, *361*, 661−674.
(3) Strydom, D. J. Snake Venom Toxins. The Amino Acid Sequences of Two Toxins from Dendroaspis Polylepis Polylepis (Black Mamba). *J. Biol. Chem.* **1972**, *247*, 4029−4042.
(4) Harvey, A. L.; Anderson A. J.; Karlsson, E. Facilitation of Transmitter Release by Neurotoxins from Snake Venoms. *J. Physiol.* (*Paris*) **1984**, *79*, 222−227.
(5) Docherty, R. J.; Dolly J. O.; Halliwell, J. V.; Othman, I. B. Excitatory Effects of Dendrotoxin on the Hippocampus in vitro. *J. Physiol. (London)* **1983**, *336*, 58P−59P.
(6) Dolly, J. O.; Halliwell, J. V.; Black J. D.; Williams R. S.; Pelchen-Mathews A.; Breeze A. L.; Mehraban F.; Othman I. B.; Black A. R. Botulinum Toxin and Dendrotoxin as Probes for Studies on Transmitter Release. *J. Physiol.* (*Paris*) **1984**, *79*, 280−303.
(7) Dolly, J. O.; Stansfeld, C. E.; Breeze, A. L.; Pelchen-Matthews, A.; Marsh, S. J.; Brown, D. A. In *Neurotoxins and Their Pharmacological Implications*; Jenner, P., Ed.; Raven Press: New York, 1987; pp 81−96.
(8) Halliwell, J. V.; Othman, I. B.; Pelchen-Mathews, A.; Dolly, J. O. Central Action of Dendrotoxins: Selective reduction of a transcient current K conductance in Hippocampus and binding to localized acceptors. *Proc. Natl. Acad. Sci. U.S.A.* **1986**, *83*, 493−497.
(9) Penner, R.; Petersen, M.; Pierau, F.-K.; Dreyer F. Dendrotoxin: A Selective Blocker of a Non-inactivating Potassium Current in Guinea-pig Dorsal Root Ganglion Neurones. *Pflugers Arch Eur. J. Physiol.* **1986**, *407*, 365−369.
(10) Benoit, E.; Dubois J. M. Toxin I from the Snake Dendroaspis Polylepis Polylepis: a Highly Specific Blocker of One Type of Potassium Channel in Mylinated Nerve Fiber. *Brain Res.* **1986**, *377*, 374−377.
(11) Black, A. R.; Breeze, A. L.; Othman, I. B.; Dolly, J. O. Involvement of Neuronal Acceptors for Dendrotoxin in its Convulsive Action in Rat Brain. *Biochem. J.* **1986**, *237*, 397−404.
(12) Dreyer, F.; Penner, R. The Actions of Presynaptic Snake Toxins on Membrane Currents of Mouse Motor Nerve Terminals. *J. Physiol. (Paris)* **1987**, *386*, 445−463.
(13) Rowan, E. G.; Harvey, A. L. Potassium Channel Blocking Actions of β-bungarotoxin and Related Toxins on Mouse and Frog Motor Nerve Terminals. *Br. J. Pharmacol.* **1988**, *94*, 839−847.
(14) Stansfeld, C. E.; Marsh, S. J.; Parcej, D. N.; Dolly, J. O.; Brown, D. A. Mast-Cell Degranulating Peptide and Dendrotoxin Selectively Inhibit a Fast-Activating Potassium Current and Bind to Common Neuronal Proteins. *Neuroscience* **1987**, *23*, 893−902.
(15) Breeze, A. L.; Dolly, J. O. Interactions Between Discrete Neuronal Membrane Binding Sites for the Putative K^+ Channel Ligands β-bungarotoxin, Dendrotoxin and Mast-Cell-Degranulating Peptide. *Eur. J. Biochem.* **1989**, *178*, 771−778.
(16) Dufton, M. J. Proteinase inhibitors and Dendrotoxins, Sequence Classification, Structural Prediction and Structure/Activity. *Eur. J. Biochem.* **1985**, *153*, 647−654.
(17) Laskowski, M.; Kato, I. Protein Inhibitors of Proteinases. *Annu. Rev. Biochem.* **1980**, *49*, 593−626.
(18) Huber, R.; Kukla, D.; Rühlmann, A.; Steigemann, W. Pancreatic trypsin Inhibitor (Kunitz). *Proc. Cold Spring Harbor Symp. Quant. Biol.* **1971**, *36*, 141−150.
(19) Wlodawer, A.; Deisenhofer, J.; Huber, R. Comparison of Two Highly Refined Crystal Structure of Bovine Pancreatic Trypsin Inhibitor. *J. Mol. Biol.* **1987**, *198*, 145−156.
(20) Deisenhofer, J.; Steigemann, W. Crystallographic Refinement of the Structure of Bovine Pancreatic Trypsin Inhibitor at 1.5 Å Resolution. *Acta Crystallogr.* **1975**, *B31*, 238−250.
(21) Mebbs, D. Snake Venom Toxins:Structural Aspects. In *Neurotoxins in Neurochemistry*; Dolly, J. O., Ed.; Ellis Horwood Ltd.: Chichester, 1988; pp 3−12.
(22) Swaminathan, P. Internal Reports of Wyeth-Ayerst Research: CN-8000, Princeton, NJ, 1988.

(23) Swaminathan, P.; Opalko, A. Molecular Structure and Conformational Analysis of Dendrotoxins and its Homologues: As Determined by Molecular Mechanics, Molecular Dynamics Techniques. *Pittsburgh Diffraction Conference 50th Annual Meeting, August 9*−14, 1992; ACA abstracts-PA42.
(24) Skarzynski, T. Crystal Structure of α-dendrotoxin from the Green Mamba Venom and its Comparison with the Structure of Bovine Pancreatic Trypsin Inhibitor. *J. Mol. Biol.* **1992**, *224*, 671−683.
(25) Foray, M.-F.; Lancelin, J.-M.; Hollecker, M.; Mation, D. Sequence Specific ^{1}H-NMR Assignment and Secondary Structure of Black Mamba Dendrotoxin I, a highly Selective Blocker of Voltage-Gated Potassium Channels. *Eur. J. Biochem.* **1993**, *211*, 813−820.
(26) Berndt, K. D.; Güntert, P.; Wüthrich, K. Nuclear Magnetic Resonance Solution Structure of Dendrotoxin-K from the Venom of Dendroaspis-polylepis-polylepis. *J. Mol. Biol.* **1993**, *234*, 735−750.
(27) SYBYL (version 6.0.3), A molecular modeling program with Interactive Graphics terminal, Tripos Associates Inc., St. Louis, MO, 1985.
(28) Singh, U. C.; Weiner, P. K.; Caldwell, J. W.; Kollman, P. A. AMBER(UCSF), version 3.0, Department of Pharmaceutical Chemistry, University of California, San Francisco, CA, 1986.
(29) Singh, U. C.; Kollman, P. A. An Approach to Computing Electrostatic Charges for Molecules. *J. Comput. Chem.* **1984**, *5*, 129−145.
(30) Singh, U. C.; Kollman, P. A. A Combined *ab initio* Quantum Mechanical and Molecular Mechanical Method for Carrying out Simulations on Complex Molecular Systems: Applications to the CH3C1+Cl$^-$ Exchange Reaction and Gas Phase Protonation of Polyethers. *J. Comput. Chem.* **1986**, *7*, 718−730.
(31) Weiner, S. J.; Kollman, P. A.; Case, D. A.; Singh, U. C.; Ghio, C.; Alagona, G.; Profeta, S.; Weiner, P. A New Force Field for Molecular Dynamics Simulation of Nucleic Acids and Proteins. *J. Am. Chem. Soc.* **1984**, *106*, 765−784.
(32) McQuarie, D. A. *Statistical Mechanics*; Harper and Row: New York, 1976.
(33) McCammon, J. A.; Harvey, S. C. *Dynamics of Proteins and Nucleic Acids*. Cambridge University Press: New York, 1988.
(34) Beveridge, D. L.; Meizei, M.; Mehrotra, P. K.; Marchese, F. T.; Ravishanker, G.; Vasu, T.; Swaminathan, S. Monte Carlo Simulation Studies of the Equilibrium Properties and Structure of Liquid Water. In *Molecular-based study of fluids*; Haile, J. M., Mansoori, G. A., Eds.; American Chemical Society: Washington, DC, 1983; pp 297−351.
(35) Friedman, H. L. Methods to Determine Structure in Water and Aqueous Solutions. *Methods Enzymol. Biomembranes* **1986**, *127*, 3−21.
(36) (a) Marquert, M.; Walter, J.; Deisenhofer, J.; Bode, W.; Huber, R. The Geometry of the Reactive Site and of the Peptide Groups in Trypsin, Trypsinogen and its Complexes with Inhibitors. *Acta Crystallogr.* **1983**, *B39*, 480−490. (b) Rühlmann, A.; Kukla, D.; Schwager, P.; Bartels, K.; Huber, R. Structure of the Complex Formed by Bovine Trypsin and Bovine Pancreatic Trypsin Inhibitor. *J. Mol. Biol.* **1973**, *77*, 417−436.
(37) Chen, Z.; Bode, W. Refined 2.5 Å X-ray Crystal Structure of the Complex Formed by Porcine Kallikrein A and the Bovine Pancreatic Trypsin Inhibitor. *J. Mol. Biol.* **1983**, *164*, 283−311.
(38) Chothia, C. Principles that Determine the Protein Structure. *Annu. Rev. Biochem.* **1984**, *53*, 537−572.
(39) (a) Venkatachalam, C. M. Stereochemical Criteria for Polypeptides and Proteins. V. Conformation of a System of Three Linked Peptide Units. *Biopolymers* **1968**, *6*, 1425−1436. (b) Rose, G. D.; Gierasch, L. M.; Smith, J. A. Turns in Peptides and Proteins. *Adv. Protein Chem.* **1985**, *37*, 1−109. (c) Kuntz, I. D. Protein Folding. *J. Am. Chem. Soc.* **1972**, *94*, 4009−4012.
(40) Chicheportiche, R.; Rochat, C.; Sampieri, F.; Lazdunski, M. Structure-Function Relationships of Neurotoxins Isolated from *Naje haje* Venom. Physico-Chemical Properties and Identification of the Active Site. *Biochemistry* **1988**, *11*, 1681−1690.
(41) Richardson, J. The Anatomy and Taxonomy of Protein Structure. *Adv. Protein Chem.* **1981**, *34*, 167−339.
(42) Kobayashi, Y.; Sato, A.; Takashima, H.; Tamaoki, H.; Nishimura, S.; Kyogoku, Y.; Ikenaka, K.; Kondo, T.; Mikoshiba, K.; Hojo, H.; Aimoto, S.; Moroder, L. A New Helical Motif in Membrane Active Peptides. *Neurochem. Int.* **1991**, *18*, 525−534.
(43) Harvey, A. L.; Anderson, A. J. Dendrotoxins: Snake Toxins That Block Potassium Channels and Facilitate Neurotransmitter Release. *Pharmacol. Ther.* **1985**, *31*, 33−55
(44) Weller, U.; Bernhardt, U.; Siemen, D.; Dryer, F.; Vogel, W.; Habermann, E. Electrophysiological and neurobiological evidence for the blockade of a potassium channel by dendrotoxin. *Naunyn-Schmiedebergs Arch. Pharmacol.* **1985**, *330*, 77−83.
(45) Harvey, A. L.; Anderson, A. J.; Mbugua, P. M.; Karlsson, E. Toxins from mamba venom that facilitate neuromuscular transmission. *J. Toxicol. Toxin Rev.* **1984**, *3*, 91−137.
(46) (a) Hollecker, M.; Marshall D. L.; Harvey, A. L. Structural Features Important for Activity of the Potassium Channel Blocking Dendrotoxins. *Br. J. Pharmacol.* **1993**, *110*, 790−794. (b) Hollecker, M.; Larcher, D. Conformational Forces Affecting the Folding Pathways of Dendrotoxins I and K from Black Mamba Venom. *Eur. J. Biochem.* **1989**, *179*, 87−94.
(47) Hurst, R. S.; Busch, A. E.; Kavanaugh, M. P.; Osborne, P. B.; North, R. A.; Adelman, J. P. Identification of Amino Acids Residues Involved in Dendrotoxin Block of Rat Voltage-Dependent Potassium Channels. *Mol. Pharmacol.* **1991**, *40*, 572−576.
(48) Miller, C. Annus Mirabilis of Potassium Channels. *Science* **1990**, *252*, 1092−1096.
(49) Hille, B. *Ionics Channels of Excitable Membranes*; Sinauer Associates Inc.: Sunderland, MA, 1984.
(50) Yool, A. J.; Schwarz, T. L. Alteration of Ionic Selectivity of a K^+ Channel by Mutation of the H5 Region. *Nature* **1991**, *349*, 700−704.
(51) Sato, K.; Ishida, Y.; Wakamatsu, K.; Kato, R.; Honda, H.; Ohizumi, Y.; Nakamura, H.; Ohya, M.; Lancelin, J.; Kohda, D.; Inagaki, F. Active Site of μ-Conotoxin GIIA, a Peptide Blocker of Muscle Sodium Channels. *J. Biol. Chem.* **1991**, *266*, 16989−16991.
(52) Chothia, C.; Finkelstein, A. V. The Classification and Origins of Protein Folding. *Annu. Rev. Biochem.* **1990**, *59*, 1007−1039.
(53) Werkman, T. R.; Gustafson, T. A.; Rogowski, R. S.; Blaustein, M. P.; Rogawski, A. Tityustoxin-Kα, a Structurally Novel and Highly Potent K^+ Channel Peptide Toxin, Interacts with α-dendrotoxin Binding Site on the Cloned Kv1.2K^+ Channel. *Mol. Pharmacol.* **1993**, *44*, 430−436.
(54) Lancelin, J.-M.; Khoda, D.; Tate, S.; Yanagawa, Y.; Abe, T.; Satake, M.; Inagaki, F. Tertiary Structure of Conotoxin GIIIA in Aqueous Solution. *Biochemistry* **1991**, *30*, 6908−6916.
(55) Benishin, C. G.; Sorensen, R. G.; Brown, W. E.; Krueger, B. K.; Blaustein, M. P. Four Polypeptide Components of Green Mamba Venom Selectively Block Certain Potassium Channels in Rat Brain Synaptosomes. *Mol. Pharmacol.* **1988**, *34*, 152−159.
(56) Kaiser, E. T.; Kezdy, F. J. Secondary Structures of Proteins and Peptides in Amphiphilic Environments (A Review). *Proc. Natl. Acad. Sci. U.S.A.* **1983**, *80*, 1137−1143.
(57) (a) Strong, P. N. Potassium Channel Toxins. *Pharmacol. Ther.* **1990**, *46*, 137−162. (b) Rehm, H.; Bidard, J. N.; Hugues, S.; Lazdunski, M. The Receptor Site for Bee Venom Mast-Cell Degranulating Peptide. Affinity Labelling and Evidence for a Common Molecular Target for Mast-Cell Degranulating Peptide and Dendrotoxin I, a Snake Toxin Active on K^+ Channels. *Biochemistry* **1988**, *27*, 1827−1832.
(58) IUPAC−IUB Commission on Biochemical Nomenclature. Abbreviations and Symbols for the Description of the Conformation of the Poly-Peptide Chains. *J. Mol. Biol.* **1970**, *52*, 1−17.
(59) Laskowski, R. A. PROCHECK: A Program to Check the Stereochemical Quality of Protein Structures. *J. Appl. Crystallogr.* **1993**, *26*, 283−291.
(60) Kraulis, P. MOLSCRIPT: A Program to Produce Both Detailed and Schematic Plots of Protein Structures. *J. Appl. Crystallogr.* **1991**, *24*, 946−950.

JM950579P